IOPscience iopscience.iop.org

Home Search Collections Journals About Contact us My IOPscience

Quantum carpets: a tool to observe decoherence

This article has been downloaded from IOPscience. Please scroll down to see the full text article.

2013 New J. Phys. 15 013052

(http://iopscience.iop.org/1367-2630/15/1/013052)

View the table of contents for this issue, or go to the journal homepage for more

Download details:
IP Address: 130.39.183.185
The article was downloaded on 22/01/2013 at 16:56

Please note that terms and conditions apply.

New Journal of Physics
The open access journal for physics

Quantum carpets: a tool to observe decoherence

P Kazemi[1], **S Chaturvedi**[2], **I Marzoli**[3,5], **R F O'Connell**[4] **and W P Schleich**[1]

[1] Institut für Quantenphysik and Center for Integrated Quantum Science and Technology (IQ^{ST}), Universität Ulm, D-89069 Ulm, Germany
[2] School of Physics, University of Hyderabad, Hyderabad 500 056, India
[3] School of Science and Technology, Università di Camerino, I-62032 Camerino, Italy
[4] Department of Physics and Astronomy, Louisiana State University, Baton Rouge, LA 70803-4001, USA
E-mail: irene.marzoli@unicam.it

New Journal of Physics **15** (2013) 013052 (18pp)
Received 9 August 2012
Published 21 January 2013
Online at http://www.njp.org/
doi:10.1088/1367-2630/15/1/013052

Abstract. Quantum carpets—the spatio-temporal de Broglie density profiles—woven by an atom or an electron in the near-field region of a diffraction grating bring to light, in real time, the decoherence of each individual component of the interference term of the Wigner function characteristic of superposition states. The proposed experiments are feasible with present-day technology.

[5] Author to whom any correspondence should be addressed.

Content from this work may be used under the terms of the Creative Commons Attribution-NonCommercial-ShareAlike 3.0 licence. Any further distribution of this work must maintain attribution to the author(s) and the title of the work, journal citation and DOI.

© IOP Publishing Ltd and Deutsche Physikalische Gesellschaft

Contents

1. Introduction **2**
2. Quantum carpets woven by Wigner functions **4**
2.1. Carpet represented as a superposition of Wigner function components 4
2.2. Schrödinger cats 6
2.3. Quantum carpet for a Schrödinger cat 6
3. Quantum carpets in the presence of decoherence **7**
3.1. Decoherence due to spontaneous emission 7
3.2. Decoherence due to image charges 10
3.3. Discussion 13
4. Summary and outlook **13**
Acknowledgments **14**
Appendix. The Wigner function corresponding to a periodic array of wave functions **14**
References **16**

1. Introduction

Decoherence [1] is an essential ingredient of quantum mechanics. Very often it is used to explain the emergence of the classical world [2–5] from a microscopic level. However, even macroscopic molecules [6–8] such as C_{60}, C_{70}, $C_{60}F_{48}$ or $C_{44}H_{30}N_4$ and interacting atomic Bose–Einstein condensates [9] display interference properties.

Although in experiments involving a cavity field [10–12], superconducting quantum circuits [13], an ion stored in a Paul trap [14], C_{70} fullerenes [15] and a neutron in an interferometer [16] one has observed certain features of the decoherence of Fock states or of the superposition of two coherent states [17], the quest [18] to record the decay of the total Wigner function [19] of such non-classical states remains an important issue in studies in quantum mechanics. In the present work, we show that the space–time structures in the position probability distribution of a de Broglie wave after a diffraction grating, i.e. quantum carpets [20], allow us to observe the decay of each individual component of the Wigner function in real time.

Under appropriate conditions the quantum mechanical probability density of a non-relativistic particle displays [20], when represented in space–time, characteristic valleys and ridges as shown in figure 1. These striking patterns have led to the name *quantum carpet*. Its design is most pronounced when the energy spectrum, determining the propagation of the particle, produces a strong degeneracy of intermode traces [21], as is the case for the particle caught in a box [22] or diffracted from an infinite periodic grating. The latter situation is closely related to the Talbot effect [20, 22]. Moreover, some features, such as the full and fractional revivals, also persist in the presence of small relativistic corrections [23] or even in a fully relativistic case [24], described by the Dirac equation. The ridges and valleys do not follow classical trajectories but the world lines created by interference. Consequently, the design of the carpet is purely an interference effect and is, therefore, sensitive to decoherence.

We show that a quantum carpet in the presence of decoherence allows us to observe the decay of each momentum component of the interference Wigner contribution. Our proposal relies on three guiding principles: (i) a quantum carpet, which is the position probability density $P(x, t)$ to find the particle at the transverse position x at a distance $z = v_z t$ after a diffraction

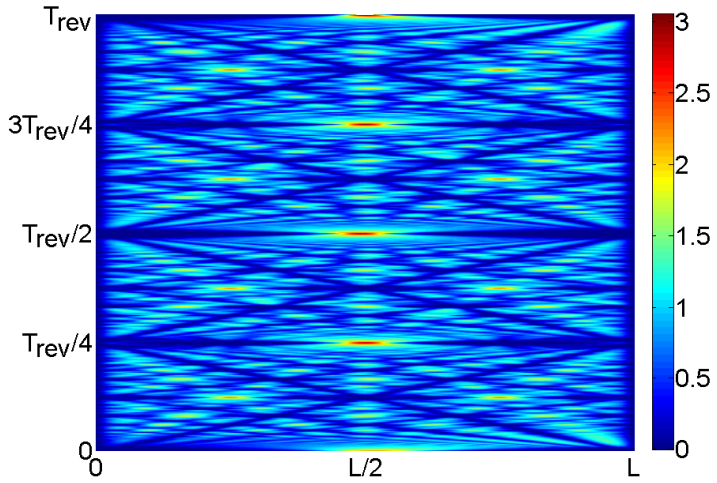

Figure 1. Quantum carpets in the absence of decoherence represented by the position probability density $P(x, t)$ of a beam of atoms or electrons after it has been diffracted from a grating aligned along the x-axis. To enhance the pattern visibility, the plot is in the logarithmic scale. Bright or dark colours represent high or low probability densities as indicated by the thermometer located on the right-hand side of the figure. Time translates into distance $z = v_z t$ from the grating by the macroscopic velocity v_z of the beam orthogonal to the x-axis. Here we have chosen an initial Gaussian wave packet centred in $\bar{x} = L/2$, having an average momentum $\bar{p} = 10\hbar/L$ and width $\Delta x = 0.03L$.

grating, is given by an incoherent sum of the Wigner functions at the grating [22], (ii) a diffraction grating can create a superposition state and (iii) de Broglie waves based on atoms and electrons provide a variety of mechanisms of decoherence [25].

We consider two types of carpets corresponding to two distinctly different mechanisms of decoherence: a carpet woven by (i) a two-level atom that can spontaneously go to its ground state and thereby receives a single random momentum kick, and (ii) an electron that passes close to a metal plate and thereby gets damped by its image charge and undergoes Brownian motion. In both cases the design of the carpet gets washed out as the distance to the grating increases.

Present-day technology even allows us to implement our proposal. Indeed, quantum carpets for several types of de Broglie waves [26–31] and of light [32] have been observed. Moreover, the influence of a single spontaneously emitted photon on the far-field interference pattern of an atomic wave has been measured [33]. Likewise, the field of electron optics [34, 35] has made remarkable progress and a double-slit experiment in the presence of a metal plate has already been carried out [36] at the University of Tübingen. Hence, the proposed observation of the space–time patterns in the probability density can serve as a flexible tool to monitor decoherence in a variety of experimental settings and conditions. A deeper understanding of decoherence not only is of interest to investigate the quantum to classical transition, but also has practical implications for the development of reliable quantum technologies.

This paper is organized as follows. In section 2 we connect the design of a quantum carpet to the individual components of the initial Wigner function. We then, in section 3, consider two different mechanisms of decoherence and study their effect on the space–time structures of the

probability density. Finally, we summarize and discuss our results in section 4. For technical details of the derivation of the Wigner function produced by a periodic array of wave functions, see the appendix.

2. Quantum carpets woven by Wigner functions

We start our discussion by connecting the design of a carpet to the individual components of the initial Wigner function. For this purpose, we study the diffraction of a non-relativistic quantum mechanical particle from a grating and emphasize that many such experiments have been performed with atoms [26–28], molecules [8], electrons [29–31, 36], neutrons [16] or light [32].

2.1. Carpet represented as a superposition of Wigner function components

Here we express the probability density in space–time forming the quantum carpet as an infinite superposition of Wigner functions corresponding to an array of Schrödinger cat states. This state corresponds to the initial state. The time dependence enters as a displacement of the original Wigner function along straight lines in space–time.

A mechanical or optical grating of period $2L$ produces a periodic array

$$\psi(x; t=0) \equiv \sum_{l=-\infty}^{\infty} \phi(x - 2lL) \tag{1}$$

of wave functions. Here x denotes the coordinate along the grating and $\phi = \phi(x)$ is the wave packet created by a single slit.

When we substitute this wave function into the definition [19]

$$W(x, p; t) \equiv \frac{1}{2\pi\hbar} \int_{-\infty}^{\infty} \mathrm{d}\xi\, \psi\left(x + \frac{1}{2}\xi, t\right) \psi^*\left(x - \frac{1}{2}\xi, t\right) \mathrm{e}^{-\mathrm{i}p\xi/\hbar} \tag{2}$$

of the Wigner function, we find in view of the results obtained in the appendix that the Wigner function

$$W_\psi(x, p; t=0) = \frac{\pi\hbar}{2L} \sum_{n,l} (-1)^{nl} \delta(p - p_n)\, W_\phi(x - lL, p_n) \tag{3}$$

of such an array with period $2L$ consists of a periodic array of Wigner functions

$$W_\phi(x, p) \equiv \frac{1}{2\pi\hbar} \int_{-\infty}^{\infty} \mathrm{d}\xi\, \phi\left(x + \frac{1}{2}\xi\right) \phi^*\left(x - \frac{1}{2}\xi\right) \mathrm{e}^{-\mathrm{i}p\xi/\hbar} \tag{4}$$

separated by L.

Due to the spatial periodicity, the momentum

$$p_n \equiv n\frac{\pi\hbar}{2L} \tag{5}$$

is discrete. We also note, in (3), the presence of the alternating weight factor $(-1)^{n\cdot l}$ for the individual contributions of the Wigner function.

After the grating the particle evolves freely as expressed by the Liouville equation [19]

$$\hat{\mathcal{L}}\, W_\psi(x,\, p;\, t) = 0, \tag{6}$$

where

$$\hat{\mathcal{L}} \equiv \frac{\partial}{\partial t} + \frac{p}{M}\frac{\partial}{\partial x} \tag{7}$$

denotes the Liouville operator of free motion for a particle of mass M. It is easy to verify that the expression

$$W_\psi(x,\, p;\, t) = W_\psi\left(x - \frac{p}{M}t,\, p;\, t = 0\right) \tag{8}$$

in terms of the initial Wigner function is the solution of the Liouville equation (6).

With the help of expression (3), we find that

$$W_\psi(x,\, p;\, t) = \frac{\pi\hbar}{2L}\sum_{n,l}(-1)^{nl}\delta(p - p_n)\, W_\phi\left[\chi_{n,l}(x,t),\, p_n\right] \tag{9}$$

with the straight space–time trajectories

$$\chi_{n,l}(x,t) \equiv x - \frac{p_n}{M}t - lL. \tag{10}$$

The position distribution $P(x,t)$ at a distance $z \equiv v_z t$ from the grating forms the carpet. Here v_z is the velocity component orthogonal to the grating. Since definition (2) of the Wigner function implies the identity

$$P(x,t) = \int_{-\infty}^{\infty} \mathrm{d}p\, W_\psi(x,\, p;\, t), \tag{11}$$

we find $P(x,t)$ from (9) by integration over p, which yields

$$P(x,t) = \frac{\pi\hbar}{2L}\sum_{n,l}(-1)^{nl} W_\phi\left[\chi_{n,l}(x,t),\, p_n\right]. \tag{12}$$

Hence, the cut of the Wigner distribution along the x-axis for a fixed momentum p_n moves along the straight space–time trajectory $\chi_{n,l}$ with a fixed speed determined by p_n. Thus as time increases, the individual cuts of the Wigner distribution at neighbouring momenta separate. We can distinguish them when the size of the Wigner structure is smaller than the separation between two of them. The fastest separation occurs for almost vertical space–time trajectories, that is, for small momenta contained in the Wigner function of the original state. Small momenta are usually a characteristic feature of superposition states.

A consequence of momentum quantization is the periodic revival of the probability density $P(x,t)$. Indeed, there exists a revival time T_1 such that $P(x, t+T_1) = P(x,t)$. This rephasing takes place when all components of the Wigner functions $W_\phi[\chi_{n,l}(x,t),\, p_n]$ have travelled a transverse distance, which is an integer multiple of the period $2L$ of the grating. Therefore, the revival time is set by the smallest momentum component $p_1 \equiv \pi\hbar/(2L)$, that is, by

$$T_1 \equiv \frac{2L}{p_1/M} = \frac{4L^2 M}{\pi\hbar}. \tag{13}$$

2.2. Schrödinger cats

Next we recall [17] the Wigner function corresponding to the anti-symmetric superposition

$$\phi(x) \equiv \varphi(x) - \varphi(-x), \tag{14}$$

built from the wave packet $\varphi = \varphi(x)$. Indeed, when we substitute this superposition into definition (2) of the Wigner function we obtain, owing to the bilinearity of W in ϕ, the expression

$$W_\phi(x, p) = W_\varphi(x, p) + W_\varphi(-x, -p) + W_{\text{int}}(x, p), \tag{15}$$

where

$$W_\varphi(x, p) \equiv \frac{1}{2\pi\hbar} \int_{-\infty}^{\infty} \mathrm{d}\xi\, \varphi\left(x + \frac{1}{2}\xi\right) \varphi^*\left(x - \frac{1}{2}\xi\right) \mathrm{e}^{-\mathrm{i}p\xi/\hbar} \tag{16}$$

represents the Wigner function of the basis packet, and the interference term W_{int} is given by

$$W_{\text{int}}(x, p) \equiv -\frac{1}{2\pi\hbar} \int_{-\infty}^{\infty} \mathrm{d}\xi \left[\varphi\left(-\left(x + \frac{1}{2}\xi\right)\right) \varphi^*\left(x - \frac{1}{2}\xi\right) + \varphi\left(x + \frac{1}{2}\xi\right) \varphi^*\left(-\left(x - \frac{1}{2}\xi\right)\right)\right] \mathrm{e}^{-\mathrm{i}p\xi/\hbar}. \tag{17}$$

Hence, the Wigner function of the superposition state (14) is the sum not only of the Wigner functions of the basis packet and its phase space inversion, that is, of $W_\varphi(x, p)$ and $W_\varphi(-x, -p)$, but also contains the term W_{int}. It is this interference term which is extremely sensitive to decoherence.

The elementary example of a Gaussian wave function

$$\varphi(x) \equiv \frac{1}{\pi^{1/4}} \frac{1}{\sqrt{\Delta x}} \exp\left[-\frac{1}{2}\left(\frac{x - \bar{x}}{\Delta x}\right)^2\right] \exp\left[\frac{\mathrm{i}\bar{p}(x - \bar{x})}{\hbar}\right] \tag{18}$$

yields the Gaussian Wigner distribution

$$W_\varphi(x, p) \equiv \frac{1}{\pi\hbar} \exp\left[-\left(\frac{x - \bar{x}}{\Delta x}\right)^2\right] \exp\left[-\left(\frac{p - \bar{p}}{\Delta p}\right)^2\right], \tag{19}$$

centred around $\bar{x}$ and momentum $\bar{p}$. Here the widths Δx and $\Delta p \equiv \hbar/\Delta x$ are measures of the extension of the quantum state in phase space indicating when the Gaussian has decayed to $1/e$.

In contrast, the interference term

$$W_{\text{int}}(x, p) = -\frac{2}{\pi\hbar} \cos\left[\frac{2}{\hbar}(\bar{p}x - p\bar{x})\right] \mathrm{e}^{-(x/\Delta x)^2}\, \mathrm{e}^{-(p/\Delta p)^2} \tag{20}$$

is always located at the origin of phase space independent of the initial position $\bar{x}$ and momentum $\bar{p}$. Moreover, it assumes negative values whereas W_φ is everywhere positive.

2.3. Quantum carpet for a Schrödinger cat

Indeed, for the example of the superposition state ϕ with a Gaussian wave packet φ of a macroscopic average momentum $\bar{p} \gg p_1$, we find a clear separation into momenta around $\bar{p}$ giving rise to rather flat trajectories in space–time and small momenta creating steep world lines.

The latter result from the interference term $W_{\rm int}$. Hence, $W_{\rm int}$ translates itself into the design of the carpet.

But how to create a superposition state such as ϕ from a grating? Many possibilities offer themselves. In the case of atoms [19], we can use an optical grating which automatically creates the desired superposition. In the case of a mechanical grating [21], we can send two de Broglie waves under an appropriate angle onto the grating. In figure 1 we show a quantum carpet woven by a particle prepared in the superposition state defined by (14) and (18). Due to the parity of the initial wave function, it suffices to study the probability density in the space region from 0 to L and up to the revival time $T_{\rm rev} = T_1/2$.

3. Quantum carpets in the presence of decoherence

We now derive expressions for quantum carpets in the presence of decoherence. Here we consider two quantum systems with different mechanisms of decoherence: (i) a two-level atom undergoing spontaneous emission and (ii) an electron moving over a metal surface creating image charges.

3.1. Decoherence due to spontaneous emission

Our discussion starts with a two-level atom moving under the influence of spontaneous emission. The Wigner functions $W_{\rm e}$ and $W_{\rm g}$ corresponding, respectively, to atoms in the excited and ground states satisfy the generalized optical Bloch equations, which describe the coupled dynamics of internal and external atomic degrees of freedom [37]

$$\hat{\mathcal{L}}\, W_{\rm e}(x,\, p;\, t) = -\gamma\, W_{\rm e}(x,\, p;\, t) \tag{21}$$

and

$$\hat{\mathcal{L}}\, W_{\rm g}(x,\, p;\, t) = \gamma \int_{-1}^{1} {\rm d}\varepsilon\; f_{\rm s}(\varepsilon)\; W_{\rm e}(x,\, p + \varepsilon\hbar k;\, t), \tag{22}$$

where γ is the rate of spontaneous emission and $\hat{\mathcal{L}}$ denotes the Liouville operator of free motion defined by (7). The term in (21) proportional to γ describes the relaxation due to spontaneous emission. Moreover, the term at the right-hand side of (22) describes the transfer of population from the excited to the ground state by spontaneous emission. The distribution $f_{\rm s} = f_{\rm s}(\varepsilon)$ with

$$\int_{-1}^{1} {\rm d}\varepsilon\; f_{\rm s}(\varepsilon) = 1 \tag{23}$$

reflects the momentum component along the x-axis.

When the atoms exit the grating at time $t = 0$ in the excited state, the solutions of these equations read

$$W_{\rm e}(x,\, p;\, t) = {\rm e}^{-\gamma t}\; W_{\psi}\left(x - \frac{p}{M}t,\, p;\, t = 0\right) \tag{24}$$

and

$$W_{\rm g}(x,\, p;\, t) = \int_{0}^{\gamma t} {\rm d}\tau\; {\rm e}^{-\tau} \int_{-1}^{1} {\rm d}\varepsilon\; f_{\rm s}(\varepsilon)\; W_{\psi}\left(x - \frac{p}{M}t - \varepsilon\delta x_{\rm s}\tau,\, p + \varepsilon\hbar k;\, t = 0\right) \tag{25}$$

with the displacement

$$\delta x_{\mathrm{s}} \equiv \frac{\hbar k}{M}\frac{1}{\gamma} \tag{26}$$

in position during the decay time $1/\gamma$ due to the recoil of the atom giving it a velocity $\hbar k/M$.

A comparison between expressions (24) and (8) for the Wigner functions $W_{\mathrm{e}}(x,\, p;\, t)$ and $W(x,\, p;\, t)$ in the excited state and the standard one shows that the influence of decoherence is just a multiplication of W by the decay factor $\exp(-\gamma t)$. As a result, we find the quantum carpet

$$P_{\mathrm{e}}^{(\mathrm{s})}(x,\, t) = \mathrm{e}^{-\gamma t} P(x,\, t) \tag{27}$$

formed by the atoms in the excited state to be the original quantum carpet, (12), in the absence of decoherence. However, its intensity decays as a function of time, that is, separation from the grating.

Next we turn to the carpet woven by the ground state atoms. For this purpose, we substitute the initial Wigner function (3) into (25) and obtain the formula

$$W_{\mathrm{g}}(x,\, p;\, t) = \frac{\pi\hbar}{2L}\sum_{n,l}(-1)^{nl}\int_0^{\gamma t}\mathrm{d}\tau\,\mathrm{e}^{-\tau}\int_{-1}^{1}\mathrm{d}\varepsilon\; f_{\mathrm{s}}(\varepsilon)\delta(p+\varepsilon\hbar k - p_n)$$
$$\times W_{\phi}\left(x - \frac{p}{M}t - lL - \varepsilon\delta x_{\mathrm{s}}\tau,\; p+\varepsilon\hbar k\right), \tag{28}$$

which after integration over momentum with the help of the delta function yields the expression

$$P_{\mathrm{g}}^{(\mathrm{s})}(x,\, t) = \frac{\pi\hbar}{2L}\sum_{n,l}(-1)^{nl}\,\overline{W}_{\phi}^{(\mathrm{s})}\left[\chi_{n,l}(x,\, t),\; p_n;\, t\right]. \tag{29}$$

Hence, while the intensity of the carpet formed by the excited atoms fades away, the carpet formed by the atoms in the ground state builds up in intensity. However, we now have to average the original Wigner function W_{ϕ} over the displacement δx_{s} due to the spontaneously emitted photon, that is,

$$\overline{W}_{\phi}^{(\mathrm{s})}(x,\, p;\, t) \equiv \mathrm{e}^{-\gamma t}\int_0^{\gamma t}\mathrm{d}\tau\,\mathrm{e}^{\tau}\int_{-1}^{1}\mathrm{d}\varepsilon\; f_{\mathrm{s}}(\varepsilon)W_{\phi}(x+\varepsilon\delta x_{\mathrm{s}}\tau,\; p). \tag{30}$$

The averaged Wigner function $\overline{W}_{\phi}^{(\mathrm{s})}$ depends explicitly on time. In particular, after a specific time the characteristic structures of the Wigner function are averaged out.

In figure 2 we illustrate these features by showing the quantum carpets for a beam of two-level atoms, initially prepared in the excited state. The left column displays the same ideal quantum carpet in the absence of decoherence ($\gamma = 0$), which we use as a benchmark and a guide to the eye. In the other columns, we gradually increase the rate of spontaneous emission from $\gamma = 1$ (centre) to $\gamma = 5$ (right). In all our numerical calculations, we set $\hbar = 1$, $L = 1$ and $M = 1$. Moreover, we choose the photon momentum $\hbar k = 1$ and use a constant distribution $f_{\mathrm{s}} = 1/2$.

In the top and bottom rows, we show the carpets corresponding to the excited and ground states, respectively. We clearly observe the exponential damping of the probability density $P_{\mathrm{e}}^{(\mathrm{s})}$ to find the atom in the excited state (top sequence) indicated by (27). Indeed, the design of the quantum carpet remains identical to the case without decoherence (left), but the contrast in the space–time structures becomes fainter as the atom moves away from the grating.

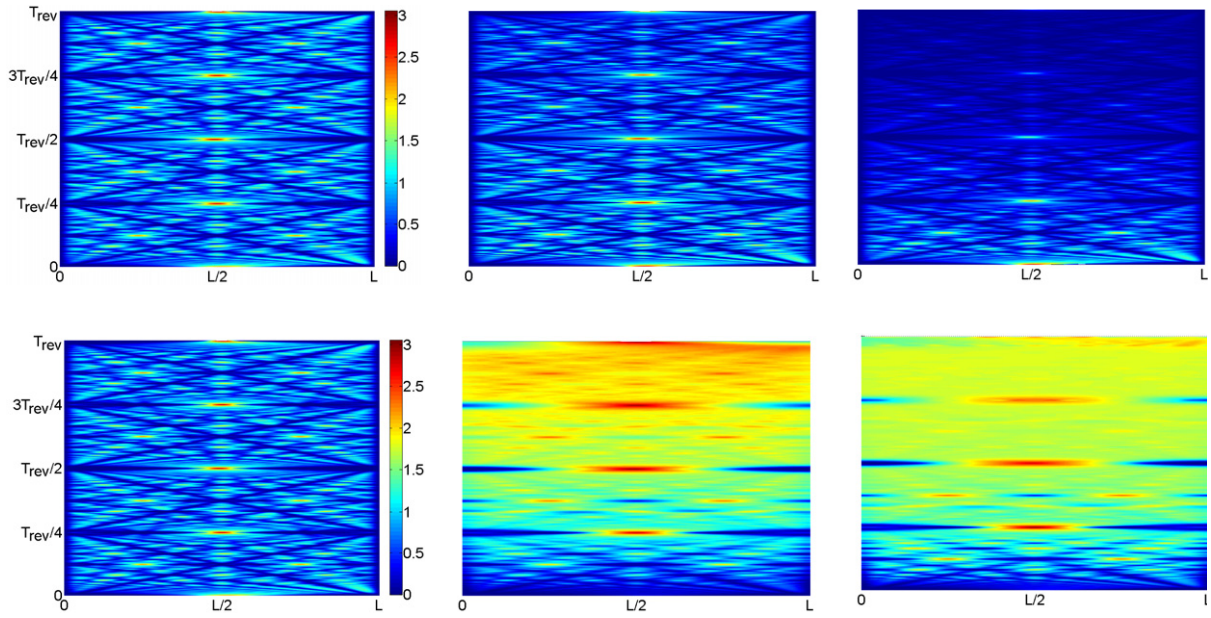

Figure 2. Decoherence of an atomic quantum carpet. Position probability density $P(x,t)$ of a beam of atoms after it has been diffracted from a grating aligned along the x-axis. To enhance the pattern visibility, the plots are in the logarithmic scale. Bright or dark colours represent high or low probability densities as indicated by the thermometer located on the right-hand side of the left figure. Time translates into distance $z = v_z t$ from the grating by the macroscopic velocity v_z of the beam orthogonal to the x-axis. The left column displays the ideal quantum carpet in the absence of decoherence ($\gamma = 0$). This plot provides us with a benchmark against which we compare the quantum carpets for increasing values of the damping rate: $\gamma = 1$ (centre) and $\gamma = 5$ (right). Top: probability density $P_{\mathrm{e}}^{(\mathrm{s})}(x,t)$ to find the atom in the excited state given by (27). Bottom: probability density $P_{\mathrm{g}}^{(\mathrm{s})}(x,t)$ to find the atom in the ground state determined by (29) and (30). Here we have chosen an initial Gaussian wave packet centred in $\bar{x} = L/2$, having an average momentum $\bar{p} = 10\hbar/L$ and a width $\Delta x = 0.03L$.

At the same time, the probability $P_{\mathrm{g}}^{(\mathrm{s})}$ of finding the atom in the ground state given by (29) and (30) (bottom centre and right) builds up in intensity. However, the random recoil due to spontaneous emission produces a less distinct pattern in the corresponding quantum carpets. In this case, one can only appreciate the revival of the Gaussian wave packet at $T_{\mathrm{rev}}/4$, $T_{\mathrm{rev}}/2$, $3T_{\mathrm{rev}}/4$ and T_{rev}. The pattern of the quantum carpet appears blurred already after $T_{\mathrm{rev}}/4$.

In order to obtain the carpet for the excited state, we have directly used the expression for $P_{\mathrm{e}}^{(\mathrm{s})}$, (27), and computed the series using a convergence tolerance of 10^{-4}. We found that this tolerance was sufficient to bring out the structures in the quantum carpet.

To plot $P_{\mathrm{g}}^{(\mathrm{s})}$, one could, in principle, use the analytical expression given by (29). However, in practice, we found the convergence of the series to be too slow. Thus, we numerically evaluate

the expression

$$P_{\mathrm{g}}^{(\mathrm{s})}(x,t)=\frac{\pi\hbar}{2L}\int_0^{\gamma t}\mathrm{d}\tau\int_{-1}^{1}\mathrm{d}\varepsilon\mathrm{e}^{-\tau}f_{\mathrm{s}}(\varepsilon)\sum_{n,l}(-1)^{nl}W_{\phi}\left(x-\frac{p_n-\varepsilon\hbar k}{M}t-lL-\varepsilon\delta x_{\mathrm{s}}\tau,\,p_n\right); \tag{31}$$

that is, we interchange summations and integrations. We now first perform the summation over n and l and then we average over ε and τ.

Here we use an adaptive Simpson quadrature rule to calculate the integral and an error tolerance of 10^{-4} for the convergence of the series in the integrand. We found that this procedure is sufficient to illustrate the effect of decoherence in the carpet structures.

3.2. Decoherence due to image charges

We now turn to the second model of decoherence: an electron propagates above a metal surface as it creates the quantum carpet. The image charge in the metal [38] leads to a damped Brownian motion of the electron described by the Langevin equation, i.e. a Heisenberg equation of motion for the position operator $\hat{x}(t)$ of the particle in equilibrium with a linear passive heat bath. For the case of a free particle interacting with an Ohmic bath, this equation takes on the well-known form [39]

$$\frac{\mathrm{d}^2\hat{x}}{\mathrm{d}t^2}+\Gamma\frac{\mathrm{d}\hat{x}}{\mathrm{d}t}=\frac{\hat{F}(t)}{M}. \tag{32}$$

Here Γ and $\hat{F}$ denote the damping constant and the Gaussian quantum force, respectively.

The explicit solution

$$\hat{x}(t)=\hat{x}(0)+\frac{\hat{p}(0)}{M\Gamma}\left(1-\mathrm{e}^{-\Gamma t}\right)+\hat{f}(t) \tag{33}$$

of the Langevin equation, (32), with the force operator

$$\hat{f}(t)\equiv\frac{1}{M}\int_0^t\mathrm{d}t'\int_0^{t'}\mathrm{d}t''\,\mathrm{e}^{-\Gamma(t'-t'')}\hat{F}(t'') \tag{34}$$

allows us to analyse the corresponding quantum carpet

$$P^{(\mathrm{B})}(x,t)\equiv\left\langle\delta[\hat{x}(t)-x]\right\rangle\equiv\frac{1}{2\pi}\int_{-\infty}^{\infty}\mathrm{d}k\left\langle\mathrm{e}^{\mathrm{i}k\hat{x}(t)}\right\rangle\mathrm{e}^{-\mathrm{i}kx} \tag{35}$$

in the presence of Brownian motion.

In order to evaluate the expectation value $\langle\exp[\mathrm{i}k\hat{x}(t)]\rangle$ with the time-dependent position operator $\hat{x}(t)$, we recall that the noise operator $\hat{f}(t)$ at time t commutes with the operators $\hat{x}(0)$ and $\hat{p}(0)$ of the electron at the initial time $t=0$, when it starts interacting with its image charge. Hence, the average $\exp[\mathrm{i}k\hat{x}(t)]$ factors into one over the electron and the other over the reservoir, that is,

$$\langle\mathrm{e}^{\mathrm{i}k\hat{x}(t)}\rangle=\left\langle\exp\left\{\mathrm{i}k\left[\hat{x}(0)+\left(1-\mathrm{e}^{-\Gamma t}\right)\frac{\hat{p}(0)}{M\Gamma}\right]\right\}\right\rangle\left\langle\mathrm{e}^{\mathrm{i}k\hat{f}(t)}\right\rangle. \tag{36}$$

We can perform the average of the symmetrically ordered operator pertaining to the electron using the Wigner function, (3), and arrive at

$$\langle \mathrm{e}^{\mathrm{i}k\hat{x}(t)}\rangle = \frac{\pi\hbar}{2L}\sum_{n,l}(-1)^{n\cdot l}\int \mathrm{d}x(0)\int \mathrm{d}p(0)\exp\left\{\mathrm{i}k\left[x(0)+\left(1-\mathrm{e}^{-\Gamma t}\right)\frac{p(0)}{M\Gamma}\right]\right\}$$
$$\times\,\delta\left(p(0)-p_n\right)W_\phi(x(0)-lL,\,p_n)\left\langle \mathrm{e}^{\mathrm{i}k\hat{f}(t)}\right\rangle, \tag{37}$$

which after integration over $p(0)$ using the delta function and the new integration variable $y' \equiv x(0)+(1-\mathrm{e}^{-\Gamma t})p(0)/(M\Gamma)$ reduces to

$$\langle \mathrm{e}^{\mathrm{i}k\hat{x}(t)}\rangle = \frac{\pi\hbar}{2L}\sum_{n,l}(-1)^{n\cdot l}\int \mathrm{d}y'\,\mathrm{e}^{\mathrm{i}ky'}W_\phi\left(y'-\left(1-\mathrm{e}^{-\Gamma t}\right)\frac{p_n}{M\Gamma}-lL,\,p_n\right)\left\langle \mathrm{e}^{\mathrm{i}k\hat{f}(t)}\right\rangle. \tag{38}$$

In the final step, we substitute this expression into the space–time distribution (35) for the carpet and find that

$$P^{(\mathrm{B})}(x,t) = \frac{\pi\hbar}{2L}\sum_{n,l}(-1)^{nl}\int \mathrm{d}y W_\phi\left(\chi^{(\mathrm{B})}_{n,l}(x,t)+y,\,p_n\right)\frac{1}{2\pi}\int \mathrm{d}k\,\mathrm{e}^{\mathrm{i}ky}\left\langle \mathrm{e}^{\mathrm{i}k\hat{f}(t)}\right\rangle, \tag{39}$$

where we have introduced $y \equiv y' - x$ and the space–time trajectory

$$\chi^{(\mathrm{B})}_{n,l}(x,t) \equiv x - \frac{p_n}{M\Gamma}\left(1-\mathrm{e}^{-\Gamma t}\right) - lL, \tag{40}$$

which is curved due to the damping.

It is convenient to arrange the terms in the form

$$P^{(\mathrm{B})}(x,t) = \frac{\pi\hbar}{2L}\sum_{n,l}(-1)^{nl}\overline{W}^{(\mathrm{B})}_\phi\left[\chi^{(\mathrm{B})}_{n,l}(x,t),\,p_n;\,t\right] \tag{41}$$

with the averaged Wigner function

$$\overline{W}^{(\mathrm{B})}_\phi(x,\,p;\,t) \equiv \int_{-\infty}^{\infty}\mathrm{d}y\;W_\phi(x+y,\,p)\,\mathcal{K}(y;\,t) \tag{42}$$

and the time-dependent kernel

$$\mathcal{K}(y;\,t) \equiv \frac{1}{2\pi}\int_{-\infty}^{\infty}\mathrm{d}k\,\mathrm{e}^{\mathrm{i}ky}\left\langle \mathrm{e}^{\mathrm{i}k\hat{f}(t)}\right\rangle \tag{43}$$

of Brownian motion.

Hence, the Brownian motion averages the initial Wigner function over a time-dependent kernel $\mathcal{K}$ and the characteristic interference features of the Wigner function disappear.

The similarities and differences between the carpets of spontaneous emission and Brownian motion stand out most clearly in the classical limit where $\mathcal{K}$ reduces to a Gaussian [5, 39]

$$\mathcal{K}(y;\,t) \equiv \frac{1}{\sqrt{\pi}\,\delta x_{\mathrm{B}}(t)}\exp\left[-\left(\frac{y}{\delta x_{\mathrm{B}}(t)}\right)^2\right], \tag{44}$$

with a time-dependent width

$$[\delta x_{\mathrm{B}}(t)]^2 \equiv \frac{D}{\Gamma}\left[2\Gamma t - 2\left(1-\mathrm{e}^{-\Gamma t}\right)-\left(1-\mathrm{e}^{-\Gamma t}\right)^2\right] \tag{45}$$

and $D \equiv k_{\mathrm{b}}T/(M\Gamma)$. Here, k_{b} and T denote Boltzmann's constant and the temperature of the metal surface, respectively.

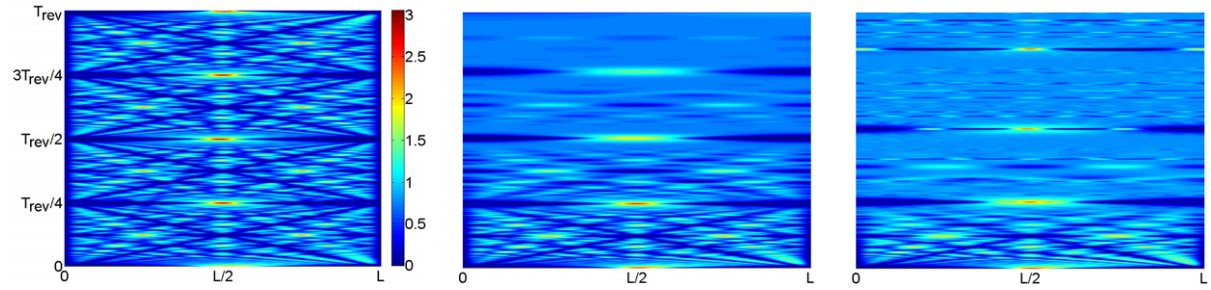

Figure 3. Decoherence of an electronic quantum carpet. Position probability density $P^{(\mathrm{B})}(x,t)$ of a beam of electrons propagating on top of a metal surface after it has been diffracted from a grating aligned along the x-axis. To enhance the pattern visibility, the plots are in the logarithmic scale. Bright or dark colours represent high or low probability densities, respectively, as indicated by the thermometer located on the right-hand side of the left figure. Time translates into distance $z = v_z t$ from the grating by the macroscopic velocity v_z of the beam orthogonal to the x-axis. Moving from left to right, we increase the damping rate from $\Gamma = 0$ to $\Gamma = 0.1$ and 0.5. Here we have chosen an initial Gaussian wave packet centred at $\bar{x} = L/2$, having an average momentum $\bar{p} = 10\hbar/L$ and a width $\Delta x = 0.03L$. The other parameters are $k_{\mathrm{b}} = 1$ and $T = 4$.

At first glance, it might appear that this result is different from the corresponding results in [4]. However, the work by Ford *et al* [4] is concerned with 'entanglement at all times', in which case no divergences appear, even at zero temperature.

On the other hand, the work by Ford and O'Connell [5] is concerned with the solution of the exact master equation (which was shown to be equivalent to the solution of the Langevin equation for the initial value problem) and, in this case, it was shown that serious divergences arise for low bath temperatures. However, as stressed in the abstract of this paper, worthwhile results may be obtained for high temperatures but one must distinguish between two cases: (a) a particle at zero (or low) temperature which is suddenly coupled to a bath at high temperature and (b) a particle whose initial temperature is the same as the bath temperature (the case where the initial temperature and the bath temperature are both high but different was not analysed in detail but it follows closely the analysis for the previous case).

It is scenario (a) that is relevant in the present context, where we envisage an electron at a relatively low temperature being brought into the confines of a metal surface at a much higher temperature.

When we substitute the Gaussian kernel (44) into (42), we find the averaged Wigner function

$$\overline{W}_{\phi}^{(\mathrm{B})}(x,\,p;\,t) = \int_{-\infty}^{\infty} \mathrm{d}\varepsilon f_{\mathrm{B}}(\varepsilon) W_{\phi}\left(x + \varepsilon\delta x_{\mathrm{B}}(t),\,p\right) \tag{46}$$

due to the Brownian motion, with the Gaussian weight function

$$f_{\mathrm{B}}(\varepsilon) \equiv \frac{1}{\sqrt{\pi}} \exp\left(-\varepsilon^2\right).$$

In figure 3 we show the probability density $P^{(\mathrm{B})}(x,t)$ to find the electron at a transverse position x and a distance $v_z t$ from the grating given by (41) and (46). The left column displays again the

ideal quantum carpet in the absence of decoherence. We then increase the value of the damping rate from $\Gamma = 0.1$ (middle) to $\Gamma = 0.5$ (right). As a result the Brownian motion quickly destroys the space–time structures in $P^{(\mathrm{B})}(x, t)$ and after $T_{\mathrm{rev}}/2$ the design of the quantum carpet gets completely washed out.

3.3. Discussion

We conclude by comparing the quantum carpets of an atom undergoing spontaneous emission and an electron moving over a metal surface. According to (46) the averaged Wigner function $\overline{W}_{\phi}^{(\mathrm{B})}$ due to Brownian motion takes a form similar to the distribution $\overline{W}_{\phi}^{(\mathrm{s})}$ defined in (30) and originating from spontaneous emission. However, there are three major differences: (i) whereas $\overline{W}_{\phi}^{(\mathrm{s})}$ contains two averages—one over the decay time and one over the momentum change—$\overline{W}_{\phi}^{(\mathrm{B})}$ involves only the average over the displacement in position. (ii) The weight function f_{B} of the Brownian motion is always a Gaussian, whereas the corresponding distribution f_{s} of spontaneous emission depends on the type of the transition and ranges from being constant to a trigonometric function. (iii) The displacement δx_{s} of spontaneous emission in (30) is linear in time for all times. In contrast, the displacement squared $[\delta x_{\mathrm{B}}]^2$ of Brownian motion, (45), grows for $\Gamma t \ll 1$ as t^3 but only turns into a linear dependence for $\Gamma t \to \infty$.

4. Summary and outlook

In conclusion, we have analysed the influence of decoherence on quantum carpets woven by de Broglie waves. Spontaneous emission or Brownian motion, the sources of decoherence, manifest themselves directly in the destruction of the design of the carpet. In this way, we can observe in real time the decay of the interference terms of the Wigner function.

We emphasize that the proposed technique to bring out the influence of decoherence is fundamentally different from the one used in the landmark experiments using photons in a cavity [10–12], an ion stored in a trap [14] or the circuit QED analogues [13]. Whereas they require the reconstruction [40, 41] of the Wigner function from measurements, such as the occupation probabilities of atomic, phononic or photonic states, the present method of using a quantum carpet measures directly the parts of the Wigner function most susceptible to decoherence. Indeed, here we take advantage of three facts: (i) we can prepare a de Broglie wave in an array of superposition states corresponding to a Schrödinger cat by diffracting it from a grating, (ii) the free propagation of the matter wave after the grating forming the carpet is classical when described by the Wigner function of the array of superposition states and (iii) the design of the carpet is intimately connected to the shape of the interference terms in the Wigner function.

Indeed, the structures of the individual world lines with their valleys and crests criss-crossing the carpet are the Wigner function components of the interference term caused by the superposition state at a given low momentum. Since we consider an infinitely long periodic grating, these momenta are discrete and structure develops in the carpet only at discrete inclinations with respect to the axes defining space–time, that is, in the near-field diffraction pattern.

Decoherence attacks predominantly the interference terms of the Wigner function and thereby fills the valleys. As a result, the design of the carpet gets washed out. However, it is

only due to the discreteness of the momenta and the time evolution of a free particle after the grating that these components separate in the form of a fan and we can observe the *filling-up* of each component.

Our proposal to use the design of a quantum carpet as a tool to observe decoherence is particularly suited for diffraction experiments such as the pioneering ones based on atoms [42], large molecules [6–8, 15, 25], light [32] or electrons [36]. Although most of these articles have analysed the apparent decoherence based on specific models, they have not made use of the direct connection between the near-field diffraction pattern defining the carpet and the Wigner function. However, it is in this way that we gain deeper insight into the nature of decoherence and, in particular, in crossing the border between the microscopic and the macroscopic world.

Acknowledgments

This project was supported by the German Space Agency DLR with funds provided by the Federal Ministry of Economics and Technology (BMWi) under grant number DLR 50WM 0837. We are also grateful to the Baden–Württemberg Stiftung for the initial funding within the programme 'Quanteninformationsverarbeitung' and the Alexander von Humboldt-Stiftung. The work of RFOC was partially supported by the National Science Foundation under grant number ECCS-1125675.

Appendix. The Wigner function corresponding to a periodic array of wave functions

In this appendix, we derive an expression for the Wigner function corresponding to an array

$$\psi(x) = \sum_{l=-\infty}^{\infty} \phi(x - 2lL) \tag{A.1}$$

of wave functions with period $2L$. Here we make no assumptions on ϕ except that it is integrable. Moreover, for simplicity in notation throughout this appendix the summation indices run over all integers and the integrals have the limits $-\infty$ and $+\infty$.

When we substitute the wave function ψ given by (A.1) into definition (2) of the Wigner function, we find that

$$W_\psi(x, p) = \frac{1}{2\pi\hbar} \sum_{k,l} \int \mathrm{d}\xi\, \phi\left(x - 2kL + \frac{1}{2}\xi\right) \phi^*\left(x - 2lL - \frac{1}{2}\xi\right) \mathrm{e}^{-\mathrm{i}p\xi/\hbar}. \tag{A.2}$$

We first change the summation indices k and l to r and s, where $k - l \equiv 2r$ and $k + l \equiv 2s$ when $k - l$ and $k + l$ are both even, and $k - l \equiv 2r + 1$ and $k + l \equiv 2s + 1$ when $k - l$ and $k + l$ are both odd. After these transformations, (A.2) takes the form

$$W_\psi(x, p) = \frac{1}{2\pi\hbar}(I_\mathrm{e} + I_\mathrm{o}), \tag{A.3}$$

where

$$I_\mathrm{e} \equiv \sum_{r,s} \int \mathrm{d}\xi\, \phi\left(x - 2(s + r)L + \frac{1}{2}\xi\right) \phi^*\left(x - 2(s - r)L - \frac{1}{2}\xi\right) \mathrm{e}^{-\mathrm{i}p\xi/\hbar} \tag{A.4}$$

contains the even and

$$I_{\mathrm{o}} \equiv \sum_{r,s} \int \mathrm{d}\xi\ \phi\left(x - 2(s+r+1)L + \frac{1}{2}\xi\right) \phi^*\left(x - 2(s-r)L - \frac{1}{2}\xi\right) \mathrm{e}^{-\mathrm{i}p\xi/\hbar} \tag{A.5}$$

the odd terms.

Next we apply the Poisson summation formula [43]

$$\sum_{m=-\infty}^{\infty} g_m = \sum_{n=-\infty}^{\infty} \int_{-\infty}^{\infty} \mathrm{d}\mu\ g(\mu)\, \mathrm{e}^{2\pi \mathrm{i} n\mu}, \tag{A.6}$$

where $g(\mu)$ is an extension of the function g_m to the whole real axis, to the summation over r and obtain the expressions

$$I_{\mathrm{e}} = \sum_{n,s} \int \mathrm{d}\mu \int \mathrm{d}\xi\ \phi\left(x - 2(s+\mu)L + \frac{1}{2}\xi\right) \phi^*\left(x - 2(s-\mu)L - \frac{1}{2}\xi\right) \mathrm{e}^{-\mathrm{i}p\xi/\hbar}\, \mathrm{e}^{2\pi \mathrm{i}\mu n} \tag{A.7}$$

and

$$I_{\mathrm{o}} = \sum_{n,s} \int \mathrm{d}\mu \int \mathrm{d}\xi\ \phi\left(x - 2(s+\mu+1)L + \frac{1}{2}\xi\right) \phi^*\left(x - 2(s-\mu)L - \frac{1}{2}\xi\right) \mathrm{e}^{-\mathrm{i}p\xi/\hbar}\, \mathrm{e}^{2\pi \mathrm{i}\mu n}. \tag{A.8}$$

It is convenient to first slightly rewrite the arguments of ϕ and cast the integrals into the form

$$I_{\mathrm{e}} = \sum_{n,s} \int \mathrm{d}\mu \int \mathrm{d}\xi\ \phi\left(x - 2sL + \frac{1}{2}(\xi - 4\mu L)\right) \phi^*\left(x - 2sL - \frac{1}{2}(\xi - 4\mu L)\right) \mathrm{e}^{-\mathrm{i}p\xi/\hbar}\, \mathrm{e}^{2\pi \mathrm{i}\mu n} \tag{A.9}$$

and

$$I_{\mathrm{o}} = \sum_{n,s} \int \mathrm{d}\mu \int \mathrm{d}\xi\ \phi\left(x - (2s+1)L + \frac{1}{2}(\xi - (4\mu+2)L)\right) \times \phi^*\left(x - (2s+1)L - \frac{1}{2}(\xi - (4\mu+2)L)\right) \mathrm{e}^{-\mathrm{i}p\xi/\hbar} \mathrm{e}^{2\pi \mathrm{i}\mu n} \tag{A.10}$$

and then introduce in I_{e} and I_{o} the new integration variables $y \equiv 4\mu L$ and $(4\mu+2)L$, respectively, which yields

$$I_{\mathrm{e}} = \frac{1}{4L} \sum_{n,s} \int \mathrm{d}y \int \mathrm{d}\xi\ \phi\left(x - 2sL + \frac{1}{2}(\xi - y)\right) \times \phi^*\left(x - 2sL - \frac{1}{2}(\xi - y)\right) \mathrm{e}^{-\mathrm{i}p\xi/\hbar} \exp\left(\mathrm{i}\pi n \frac{y}{2L}\right) \tag{A.11}$$

and

$$I_{\mathrm{o}} = \frac{1}{4L} \sum_{n,s} (-1)^n \int \mathrm{d}y \int \mathrm{d}\xi\ \phi\left(x - (2s+1)L + \frac{1}{2}(\xi - y)\right) \times \phi^*\left(x - (2s+1)L - \frac{1}{2}(\xi - y)\right) \mathrm{e}^{-\mathrm{i}p\xi/\hbar} \exp\left(\mathrm{i}\pi n \frac{y}{2L}\right). \tag{A.12}$$

Here we have made use of the identity $\mathrm{e}^{\mathrm{i}\pi n} = (-1)^n$.

When we substitute (A.11) and (A.12) back into (A.3), we can combine both terms by noting that $(-1)^{n2s} = 1$ and $(-1)^{n(2s+1)} = (-1)^n$, which yields

$$W_\psi(x,\,p) = \frac{1}{4L}\frac{1}{2\pi\hbar}\sum_{l,n}(-1)^{nl}\int \mathrm{d}y \int \mathrm{d}\bar{\xi}\;\phi\left(x - lL + \frac{1}{2}\bar{\xi}\right) \times \phi^*\left(x - lL - \frac{1}{2}\bar{\xi}\right)\mathrm{e}^{-\mathrm{i}p\bar{\xi}/\hbar}\exp\left[-\mathrm{i}\left(p - n\frac{\pi\hbar}{2L}\right)\frac{y}{\hbar}\right], \tag{A.13}$$

where we have introduced the new integration variable $\bar{\xi} \equiv \xi - y$.

Next we interchange the two integrations, recall definition (2) of the Wigner function and arrive at

$$W_\psi(x,\,p) = \frac{1}{4L}\sum_{l,n}(-1)^{nl}\,W_\phi(x - lL,\,p)\int \mathrm{d}y\,\mathrm{e}^{-\mathrm{i}(p-p_n)y/\hbar}, \tag{A.14}$$

where we have defined the Wigner function

$$W_\phi(x,\,p) \equiv \frac{1}{2\pi\hbar}\int \mathrm{d}\xi\;\phi\left(x - \frac{1}{2}\xi\right)\phi^*\left(x + \frac{1}{2}\xi\right)\mathrm{e}^{-\mathrm{i}\pi\xi/\hbar} \tag{A.15}$$

of the wave function ϕ and the discrete momentum

$$p_n \equiv n\frac{\pi\hbar}{2L} \tag{A.16}$$

introduced by the periodicity of the array.

With the help of the Fourier representation

$$\frac{1}{2\pi\hbar}\int \mathrm{d}y\,\mathrm{e}^{-\mathrm{i}py/\hbar} = \delta(p) \tag{A.17}$$

of the delta function, we obtain the result

$$W_\psi(x,\,p) = \frac{\pi\hbar}{2L}\sum_{l,n}(-1)^{nl}\,W_\phi(x - lL,\,p)\,\delta(p - p_n). \tag{A.18}$$

References

[1] Zurek W H 1991 *Phys. Today* **44** 36

[2] Giulini D J W, Joos E, Zeh H D, Kiefer C, Kupsch J and Stamatescu I-O 1996 *Decoherence and the Appearance of a Classical World in Quantum Theory* (New York: Springer)

[3] Schlosshauer M 2005 *Rev. Mod. Phys.* **76** 1267
Schlosshauer M 2007 *Decoherence and the Quantum-to-Classical Transition* (Berlin: Springer)

[4] Ford G W, Lewis J T and O'Connell R F 2001 *Phys. Rev.* A **64** 032101

[5] Ford G W and O'Connell R F 2001 *Phys. Rev.* D **64** 105020

[6] Arndt M, Nairz O, Vos-Andreae J, Keller C, van der Zouw G and Zeilinger A 1999 *Nature* **401** 680

[7] Hackermüller L, Uttenthaler S, Hornberger K, Reiger E, Brezger B, Zeilinger A and Arndt M 2003 *Phys. Rev. Lett.* **91** 090408

[8] Hornberger K, Gerlich S, Haslinger P, Nimmrichter S and Arndt M 2012 *Rev. Mod. Phys.* **84** 157
[9] Gustavsson M, Haller E, Mark M J, Danzl J G, Hart R, Daley A J and Nägerl H-C 2010 *New J. Phys.* **12** 065029
[10] Brune M, Hagley E, Dreyer J, Maître X, Maali A and Wunderlich C 1996 *Phys. Rev. Lett.* **77** 4887
[11] Deléglise S, Dotsenko I, Sayrin C, Bernu J, Brune M, Raimond J M and Haroche S 2008 *Nature* **455** 510
[12] Brune M, Bernu J, Guerlin C, Deléglise S, Sayrin C, Gleyzes S, Kuhr S, Dotsenko I, Raimond J M and Haroche S 2008 *Phys. Rev. Lett.* **101** 240402
[13] Wang H *et al* 2008 *Phys. Rev. Lett.* **101** 240401
[14] Myatt C J, King B E, Turchette Q A, Sackett C A, Kielpinski D, Itano W M, Monroe C and Wineland D J 2000 *Nature* **403** 269
[15] Hornberger K, Uttenthaler S, Brezger B, Hackermüller L, Arndt M and Zeilinger A 2003 *Phys. Rev. Lett.* **90** 160401
Hackermüller L, Hornberger K, Brezger B, Zeilinger A and Arndt M 2003 *Appl. Phys.* B **77** 781
[16] Baron M, Rauch H and Suda M 2003 *J. Opt. B: Quantum Semiclass. Opt.* **8** S241
[17] Schleich W, Pernigo M and Kien F L 1991 *Phys. Rev.* A **44** 2172
[18] Raimond J M and Haroche S 2001 *Rev. Mod. Phys.* **73** 565
Bertet P, Auffeves A, Maioli P, Osnaghi S, Meunier T, Brune M, Raimond J M and Haroche S 2002 *Phys. Rev. Lett.* **89** 200402
[19] See, for example Schleich W P 2001 *Quantum Optics in Phase Space* (Weinheim: Wiley-VCH)
[20] Berry M V, Marzoli I and Schleich W P 2001 *Phys. World* **14** 39
[21] Kaplan A E, Stifter P, van Leeuwen K A H, Lamb W E Jr and Schleich W P 1998 *Phys. Scr.* **T76** 93
[22] Grossmann F, Rost J-M and Schleich W P 1997 *J. Phys. A: Math. Gen.* **30** L277
Stifter P, Leichtle C, Schleich W P and Marklof J 1997 *Z. Naturf.* **52a** 377
Marzoli I, Saif F, Bialynicki-Birula I, Friesch O M, Kaplan A E and Schleich W P 1998 *Acta Phys. Slovaca* **48** 323
Friesch O M, Marzoli I and Schleich W P 2000 *New J. Phys.* **2** 4
[23] Marzoli I, Kaplan A E, Saif F and Schleich W P 2008 *Fortschr. Phys.* **56** 967
Ghosh S and Marzoli I 2011 *Int. J. Quantum Inform.* **9** 1519
[24] Strange P 2012 *Phys. Rev. Lett.* **104** 120403
[25] Hornberger K, Sipe J E and Arndt M 2004 *Phys. Rev.* A **70** 053608
[26] Nowak S, Kurtsiefer Ch, Pfau T and David C 1997 *Opt. Lett.* **22** 1430
Schmiedmayer J, Chapman M S, Hammond T D, Lenef A, Rubenstein R A, Smith E and Pritchard D E 1995 *Phys. Rev.* A **51** R14
[27] Ryu C, Andersen M F, Vaziri A, D'Arcy M B, Grossman J M, Helmerson K and Phillips W D 2006 *Phys. Rev. Lett.* **96** 160403
[28] Mark M J, Haller E, Danzl J G, Lauber K, Gustavsson M and Nägerl H-C 2011 *New J. Phys.* **13** 085008
[29] Ahn J, Hutchinson D N, Rangan C and Bucksbaum P H 2001 *Phys. Rev. Lett.* **86** 1179
[30] Hatsuki H, Chiba H, Meier C, Girard B and Ohmori K 2009 *Phys. Rev. Lett.* **102** 103602
See also Ohmori K 2009 *Annu. Rev. Phys. Chem.* **60** 487
[31] Korneev Ph A *et al* 2012 *Phys. Rev. Lett.* **108** 223601
[32] Case W B, Tomandl M, Deachapunya S and Arndt M 2009 *Opt. Express* **17** 20966
[33] Pfau T, Spälter S, Kurtsiefer Ch, Ekstrom C R and Mlynek J 1994 *Phys. Rev. Lett.* **73** 1223
Chapman M S, Hammond T D, Lenef A, Schmiedmayer J, Rubenstein R A, Smith E and Pritchard D E 1995 *Phys. Rev. Lett.* **75** 3783
[34] See for example Hasselbach F, Kiesel H and Sonnentag P 2000 *Decoherence: Theoretical, Experimental and Conceptual Problems* ed Ph Blanchard *et al* (Heidelberg: Springer) p 201
[35] Hasselbach F 2010 *Rep. Prog. Phys.* **73** 016101
[36] Sonnentag P and Hasselbach F 2007 *Phys. Rev. Lett.* **98** 200402
[37] Tanguy C, Reynaud S and Cohen-Tannoudji C 1984 *J. Phys. B: At. Mol. Phys.* **17** 4623

[38] Anglin J R and Zurek W H 1996 *Dark Matter in Cosmology, Quantum Measurements and Experimental Gravitation* ed R Ansari *et al* (Gif-sur-Yvette: Editions Frontières) p 263
See also Anglin J R, Paz J P and Zurek W H 1997 *Phys. Rev.* A **55** 4041
[39] Ford G W, Lewis J T and O'Connell R F 1988 *Phys. Rev.* A **37** 4419
[40] Freyberger M, Bardroff P, Leichtle C, Schrade G and Schleich W P 1997 *Phys. World* **10** 41
[41] Leibfried D, Pfau T and Monroe C 1998 *Phys. Today* **51** 22
[42] Kurtsiefer Ch, Pfau T and Mlynek J 1997 *Nature* **386** 150
[43] See, for example, Courant R and Hilbert D 1937 *Methods of Mathematical Physics* (Berlin: Springer)